Pol. J. Environ. Stud. Vol. XX, No. X (XXXX), 1-12
DOI: *10.15244/pjoes/214086* ONLINE PUBLICATION DATE: 2026-02-18

Original Research

A Multi-level Ecological Security Pattern Study of Hainan Tropical Rainforest National Park from the Perspective of Ecological Quality and Landscape Risk Synergy

Jiayi Liu, Meilin Meng*, Yao Wei

School of Design, Anhui Polytechnic University, Anhui 241000, China

Received: 30 August 2025
Accepted: 08 November 2025

Abstract

Hainan Tropical Rainforest National Park (HTNP) and its surrounding areas face the dual challenges of ecological fragmentation and environmental degradation, yet few studies have quantitatively integrated Ecological Environment Quality (EEQ) and Landscape Ecological Risk (LER) to guide spatial governance. This study aims to construct a multi-level Ecological Security Pattern (ESP) that integrates EEQ and LER, providing a scientific basis for balancing conservation and development. Using multi-source remote sensing data from 2002 to 2022, GIS spatial analysis, and the Least Cumulative Resistance (LCR) model, we identified ecological source areas, corridors, and buffer zones, and validated connectivity through Ecological Risk Index (ERI) and patch aggregation indices. Results indicate a pronounced distance-decay gradient and corridors in the ERI. The 2022 ERI increased from 0.149 at 2,500 m to 0.163 at 10,000 m, whereas the 12 ecological corridor networks significantly enhanced landscape connectivity in the park's peripheral areas. The core area maintained high ecological integrity and stability, while coastal zones still exhibited high-risk fragmentation clusters associated with human expansion. Accordingly, integrating EEQ and LER coupling into ESP construction can effectively enhance ecological resilience and provide decision-making support for adaptive spatial governance of HTNP.

Keywords: Hainan Tropical Rainforest National Park, ecological security pattern, landscape ecological risk, spatial governance, buffer zone construction

*e-mail: mengshengmeng200@163.com

Introduction

HTNP serves as the core area of China's tropical rainforest conservation system. Ecological fragmentation [1] and land-use conflicts are increasingly threatening the stability of ecosystems surrounding the park [2]. While national parks play a pivotal role in biodiversity conservation, ecological security, and advancing ecological civilization [3], maintaining ecological resilience in both core zones and surrounding areas remains a significant challenge.

Existing research emphasizes the need to establish a gradient-based, networked ESP [4] to connect core and peripheral zones. This study aims to quantitatively couple EEQ with LER to guide the construction of ESPs in tropical rainforest parks, effectively addressing the cumulative effects of ecological vulnerability [5].

Research confirms that the three-tiered chain of effects – "land use type combinations-landscape spatial configurations-ecological process responses" – directly influences the stability of the ecological barrier functions of national parks [6]. Therefore, elucidating the intrinsic mechanisms underlying the evolution of multi-scale EEQ and formulating adaptive spatial governance strategies have become scientific imperatives for balancing ecological conservation and regional development.

The spatial differentiation of LER provides a direct reflection of the pressures exerted by human activities on ecosystem stability. Habitat fragmentation, impervious surface expansion, and corridor disruption reduce landscape connectivity and trigger cascading ecological responses: impeded species dispersal leads to biodiversity decline [7], ecosystem services such as surface runoff regulation are impaired [8], and the spatial propagation of ecological vulnerability is intensified [9].

Current research paradigms are shifting from single-factor sensitivity assessments to integrated, multidimensional evaluations that encompass biodiversity maintenance, ecosystem service provision, and disturbance resistance. For example, Li et al. (2019) demonstrated that urban landscape patterns and $PM_{2.5}$ pollution exhibit significant scale-dependent spatiotemporal coupling [10]; Leuven et al. (2021) revealed cascading impacts of watershed-scale landscape configuration on water quality degradation [11], and Xu et al. (2022) used GIS-based spatial modeling to quantify threshold effects of landscape fragmentation caused by mining activities [12].

Recent breakthroughs in multi-source remote sensing technologies have transformed the dynamic assessment of regional EEQ. By integrating hyperspectral, thermal infrared, and radar data, researchers have developed multidimensional evaluation frameworks combining vegetation coverage, disturbance intensity, and ecosystem functional integrity. For instance, Ding et al. (2021) proposed the EQI model, which couples NDVI, land-use intensity, and ecosystem service equivalents to characterize spatiotemporal heterogeneity of ecological health. Its application in the Fuzhou metropolitan area demonstrated high spatial resolution advantages [13]. Such remote-sensing-based multidimensional evaluations not only quantify habitat suitability [14] but also diagnose ecosystem resilience thresholds via the disturbance-recovery indices [15]. In Hainan, although the tropical monsoon climate fosters high biodiversity, the expansion of monoculture rubber plantations increased forest fragmentation by 17.3% from 2000 to 2020, reducing the ecological connectivity index below the warning threshold of 0.58. In this study, we apply the EQI model to develop an EEQ assessment system tailored to HTNP, aiming to identify ecologically sensitive degradation zones and establish spatial priorities for rainforest restoration.

Analyzing the spatiotemporal evolution of landscape fragmentation patterns and EQI in HTNP and its surrounding areas is essential for guiding ecological restoration and buffer zone establishment. Using GIS and Fragstats 4.2, we quantified the spatial distribution of landscape patterns and EEQ from 2002 to 2022. Building on traditional approaches, our innovation lies in integrating multi-source remote sensing data with the LER index to construct the ESP of HTNP and its periphery. The LCR model developed from these datasets provides a robust framework for identifying ecological corridors, buffer zones, and priority restoration areas. Specifically, this study aims to: (1) evaluate spatiotemporal changes in environmental responsiveness within the park and its adjacent regions from 2002 to 2022; (2) characterize the spatial configuration of geomorphological patterns and their ecological implications; (3) assess the correlation between topographic arrangement and environmental responsiveness over the past two decades; and (4) provide a scientific basis for building a multi-level ESP around national-level protected areas. By coupling LER with EEQ, this research offers practical insights for enhancing ecological security and promoting sustainable spatial management.

Materials and Methods

Research Area

Hainan Province, located at the southernmost tip of China, contains the HTNP (108°44′-110°04′E, 18°33′-19°14′N) in its central mountainous region. The park covers approximately 12.1% of Hainan Island's land area and represents the island's ecological apex, with the most abundant forest resources [16]. Within the national park, vegetation and fauna exhibit a well-preserved vertical zonation along the elevation gradient, while tropical natural habitats maintain a high degree of authenticity, forming a critical barrier for the island's ecological security [17]. The ecological connectivity of HTNP is essential for linking multiple protected areas – such as Bawangling, Parrot Ridge, Jianfengling,

and Wuzhishan – thereby enhancing the structural and functional integrity of the regional ecosystem [18, 19]. This connectivity supports the free migration and reproduction of rare species and enables sustainable development strategies that align with local economic activities, including water-cycle regulation, forest restoration, and sustainable agriculture. Consequently, HTNP serves as a key research area for understanding tropical ecosystem dynamics, biodiversity conservation, and sustainable development, providing valuable data to strengthen habitat-based ESPs, improve climate adaptation capacity, and advance sustainable resource management.

Data Sources

In this study, a new ESP was developed using multiple datasets, including the Chinese land-use dataset, HTNP DEM, SLOPE, ASPECT, WATERS, NDVI, LUCC, and the LER index system [20]. To ensure data consistency and accuracy, all land-use data were validated, and all datasets were uniformly projected to the Krasovsky 1940 Albers coordinate system, resampled to a spatial resolution of 30 m × 30 m, and standardized through data clipping, scale conversion, and index normalization. These steps ensured that all datasets shared the same spatial resolution and coordinate system, meeting the requirements for spatial analysis and research standards [21]. Twenty years of relevant data were processed, and EEQ was evaluated to construct an ecological quality assessment system for HTNP by refining the EQI model.

The EEQ model proposed in this study systematically quantifies regional ecological conditions through the integration of multi-source remote sensing data. The formula is defined as:

$$\mathrm{EEQ} = \frac{\mathrm{PC1} - \mathrm{PC1}_{\min}}{\mathrm{PCI}_{\max} - \mathrm{PC1}_{\min}} \quad (1)$$

$$\mathrm{PC1} = \mathrm{PCA}(\mathrm{NDVI}, \mathrm{NDBSI}, \mathrm{LST}, \mathrm{WET}, \mathrm{AI}) \quad (2)$$

where PC1 represents the first principal component derived from PCA of five core ecological indicators. NDVI: Derived from the MOD13A2 product to characterize vegetation photosynthetic activity. Normalized Difference Built-Up Index (NDBSI): Calculated using MOD09A1 bands to quantify impervious surface distribution (accessed on 5 January 2025). Land Surface Temperature (LST): Retrieved from the MOD11A1 product to reflect thermal dynamics (accessed on 5 January 2025). WET Index: Computed based on MOD09A1 spectral bands to assess surface moisture (accessed on 5 January 2025). Abundance Index (AI): Incorporated from China's Technical Criterion for Ecosystem Status Evaluation (Ministry of Ecology and Environment, https://www.mee.gov.cn/, accessed on 5 January 2025) to measure biodiversity maintenance capacity.

Methods

LER Index Construction

Using ArcGIS to construct grids of the same spatial range and referencing the "Geographic Grid" along with relevant scholarly research, this study determines an appropriate grid size based on an average patch area of 2 to 5 times the original scale [22]. The ecological risk evaluation unit is defined as a 2 km × 2 km cell, resulting in a total of 2,626 units. The ecological risk of each unit is assessed by extracting data from the center point of each grid cell. Using FRAGSTATS 4.2 software, key landscape metrics – including the landscape fragmentation index, landscape dominance index, and landscape separation index – are calculated to evaluate landscape disturbance and loss (Table 1). The landscape vulnerability index is derived from previous research findings and, after normalization, is used to compute the final LER index.

The ERI values for each evaluation unit in Hainan Province were derived using ArcGIS geostatistical analysis. These values were assigned to the centers of the risk evaluation units, and the spatial distribution of ERI across the study area was determined through Kriging interpolation. The LER was classified into five levels using the natural breakpoint method: low-risk area (ERI≤5), medium-low-risk area (5<ERI≤4), medium-risk area (4<ERI≤3), medium-high-risk area (3<ERI≤2), and high-risk area (ERI>1).

To systematically investigate the spatial gradient changes in ecological risk, this study delineated multi-level buffer zones (2,500 m, 5,000 m, 7,500 m, and 10,000 m) based on the boundaries of the core areas of national parks and calculated the average landscape ecological risk index (ERI) for each buffer zone between 2002 and 2022 (Table 2). Statistical analysis revealed that ERI values exhibited a significant linear increasing trend with increasing distance from the core zone, confirming the spatial pattern of decreasing human activity disturbance intensity with distance. By analyzing time-series data, it was found that the average ERI values for all buffer zones showed an upward trend from 2002 to 2022, reaching a peak in 2022, indicating that ecological risks in the surrounding areas have continued to intensify over the past two decades. This result provides critical quantitative evidence for identifying risk hotspots and developing differentiated spatial governance strategies in the future.

Resistance Surface Construction

The selection of resistance factors in HTNP should consider the area's unique landscape characteristics and ecological processes, ensuring the chosen factors are representative. As a result, this research establishes a holistic index framework to evaluate landscape permeability in the park's surrounding regions, structured around three primary categories: topographic

Table 1. Methodology for calculating ecological risk data.

Exponents	Notation	Landscape Ecology Implications	Calculation method	Note
Landscape Separation Index	F_i	This value ranges from (0.1) and quantifies how spatially discrete individual landscape patches are.	$F_i = \frac{A}{2A_i}\sqrt{\frac{n_i}{A}}$	n_i is the number of patches in landscape category , is the total area of landscape , and is the total area of landscape.
Landscape dominance index	DOI	Indicates the magnitude of the influence of patches on the formation and change of landscape patterns; the larger the value, the more dominant the landscape type is, and the more important the dominance of patches is in the landscape pattern.	$DOI = d \cdot \frac{A_i}{A} + e \cdot \frac{A_i}{A}$	d and e are the weights of the relative density of the landscape and the relative area of the landscape, respectively, which are 0.6, 0.4.
Landscape fragmentation index	C_i	Quantifying the degree of internal landscape fragmentation in the study area after demobilization from external disturbance.	$C_i = \frac{n_i}{A}$	n_i is the number of patches in landscape and is the area of landscape.
Landscape Intrusiveness Index	E_i	Quantifying the extent of anthropogenic disturbance to landscape patterns.	$E_{i=}aC_i + bF_i + cDOI$	b and c are the weights of the corresponding individual landscape indices, which in this study are 0.5, 0.3, and 0.2, respectively.
Landscape Vulnerability Index	V_i	It can reflect the degree of sensitivity of each landscape type when affected by changes in the external environment, and the larger the index, the higher the regional ecological risk value.	Expert ratings normalized to obtain	
Landscape loss index	R_i	Refers to the degree of loss of natural attributes of ecosystems represented by different landscape types within a region when the region is disturbed by anthropogenic or natural factors.	$R_i = E_i \cdot V_i$	
Landscape ecological risk index	ERI	Indicates the magnitude of ecological loss when different landscape types are disturbed.	$ERI = \sum_{i=1}^{n} \frac{A_{ki}}{A_k} R_i$	ERI represents the ecological risk index of landscape ; n denotes the number of landscape types; is the area of landscape type within the kth risk plot in the study area; and FFF is the total area of the kth risk plot in the study area.

features, natural landscape attributes, and human-induced disturbances. Seven key resistance factors – DEM (m), slope (°), aspect, waters, NDVI, LUCC, and LER – were selected to construct this index system. The Analytic Hierarchy Process (AHP) was employed to calculate the weightings for these factors. This involved creating a judgment matrix to subjectively evaluate each factor's impedance effect on ecological flows on a scale from 1 to 5, with 1 being equal impedance and 5 being of utmost impedance. Subsequently, the geometric mean of each row in the judgment matrix was calculated, summed, and normalized to derive the weight for each factor. Finally, consistency testing was conducted to validate the derived weight values. The specific calculation steps are outlined below:

Construct the relevant judgment matrix.

$$A = (a_{ij})_{n\times n} = \begin{bmatrix} a_{11} & a_{12} & \cdots & a_{1n} \\ a_{21} & a_{22} & \cdots & a_{2n} \\ \vdots & \vdots & \ddots & \vdots \\ a_{n1} & a_{n2} & \cdots & a_{nm} \end{bmatrix} \quad (3)$$

Let a_i, a_j (i,j = 1, 2, ..., n) represent the element, given that matrix A is an inverse matrix that is both positive and reciprocal, $a_{ij} > 0, a_{ij} = 1, a_{ij} = \frac{1}{a_{ij}}, (i, J = 1,2,\ldots, n)$.

Weighting calculation. Based on the judgment matrix, the geometric mean of the product of the scales of each layer is determined

$$a_i = \sqrt[m]{M_i}(i = 1,\ldots, n) \quad (4)$$

Table 2. Interannual changes in the average ecological risk index (ERI) at different buffer distances from the core area of the park between 2002 and 2022.

Year	Distance 2500	Distance 5000	Distance 7500	Distance 10000
2002	0.1435	0.14933	0.15432	0.15763
2007	0.14407	0.15009	0.15538	0.15853
2012	0.14351	0.14923	0.15468	0.15792
2017	0.14812	0.15447	0.15939	0.16221
2022	0.14852	0.15536	0.16044	0.16332

The computation results undergo normalization to derive the average value for each weight w_1, and the weight vector W

$$w_i = \frac{a_i}{\sum_{i=1}^{m} a_i} \quad (5)$$

Calculate the maximum characteristic root (λmax)

$$\lambda_{max} = \frac{1}{n}\sum_{i=1}^{n} \frac{A_{Wi}}{W_i} \quad (6)$$

$$CI = \frac{\lambda_{max} - n}{n-1} \quad (7)$$

$$CR = \frac{CI}{RI} \quad (8)$$

Verify its average coherence indicator CI as shown in Equation (7):

In this study: where RI denotes the consistency index, CI represents the consistency ratio, and n corresponds to the judgment moment evaluation scale [23], a coherence test is essential to validate the precision and dependability of the outcomes. For the judgment matrix A, if the consistency index (CI) is 0.1 or less, or exactly 0, the test is deemed successful. A CI value exceeding 0.1 indicates a failed test. In our calculations, the obtained consistency index was 0.0774, meeting the criterion for success [24]. These results affirm the appropriateness of the assigned weights for the ecological sensitivity evaluation factors, validating their use in subsequent assessments.

Additionally, resistance values were categorized into five levels based on existing literature and assigned numerical values ranging from 1 to 5, detailed in Table 2. The calculation of the MCR surface revealed variations in units, attributes, and value ranges among the selected resistance factors, necessitating standardization for accurate calculation. A resistance surface was generated by weighted integration of seven resistance factors (Table 3):

$$R_{total} = \sum_{i=1}^{7} w_i \times R_i \quad (9)$$

Where w_i denotes AHP-derived weights, and R_i represents normalized resistance values (1-5 scale) for each factor. Resistance values were standardized using fuzzy membership functions based on ecological process thresholds (e.g., slope >45° assigned maximum resistance).

Ecological Corridor Identification Based on MCR Model

In this study, an ecological corridor identification system for tropical islands was developed based on the minimum cumulative resistance (MCR) model, denoted as AAA in the equation [25, 26]. The core process involved three key steps: identifying ecological sources, constructing resistance surfaces, and simulating corridors. First, using the EQI, the ecological quality of the study area was classified into five grades through the natural breakpoint (Jenks) classification method. The highest-quality ecological zones, with EQI≥0.85, were designated as ecological sources. These areas, characterized by intact vegetation cover, high biodiversity, and minimal human interference, accounted for 23.6% of the study area. The integrated resistance surface was calculated and denoted as BBB. The MCR model was then applied to extract ecological corridors connecting the source areas. The fundamental Equation is as follows.

$$R_{MC} = f\min \sum_{j=n}^{i=m} \left(D_{ij} \times R_i\right) \quad (10)$$

Where R_{MC} represents the minimum cumulative resistance value, D_{ij} is the spatial distance of a species from the source site j to the landscape unit i, and R_i denotes the resistance coefficient of landscape unit i to species movement. f indicates the positive correlation between minimum cumulative resistance and ecological processes. Potential ecological corridors between source sites were identified using the minimum cumulative resistance surfaces generated in the Linkage Mapper tool, characterized by dPC_{sum} values.

Global Spatial Autocorrelation

This study employs bivariate Moran's I to investigate the spatial correlation mechanisms between ecological

risk indices and EEQ within HTNP. Unlike univariate Moran's I, which solely examines spatial clustering of single variables, bivariate Moran's I quantifies the co-variation relationships between paired variables in adjacent spatial units (e.g., coupling the distribution of high-risk zones with low environmental quality). Through global and local spatial autocorrelation analyses [27], we systematically reveal the impact intensity and spatial spillover effects of ecological risk differentiation on environmental quality [28]. The computational formula is expressed as:

$$I_{eu} = \frac{N\sum_{i}^{n}\sum_{j\neq 1}^{n} W_{ij} Z_{i}^{g} Z_{i}^{P}}{(N-1)\sum_{i}^{n}\sum_{j\neq 1}^{n} W_{ij}} \quad (11)$$

$$I'_{eu} = Z^{g}\sum_{j=1}^{n} W_{ij} Z_{ij}^{P} \quad (12)$$

In this study: I_{eu} and I'_{eu} denote the global and local bivariate Moran indices for the landscape pattern index and ecological sensitivity index, respectively. W_{ij} represents the spatial connectivity matrix using the queen-neighbour relationship approach, while Z^{g} and Z^{p} denote the average values of the local landscape pattern index and ecological sensitivity index, respectively. i and j refer to distinct study units. Moran's I value ranges from -1 to 1, where 0 denotes no spatial correlation, and values greater than 0 indicate geographic correlation. The local Moran's I assesses local spatial autocorrelation, revealing correlations between attribute values in neighboring geographic regions [29]. The spatial relationships of ecological sensitivity in the study area were categorized into "high-high", "high-low", "low-high", "low-low", and non-significant using local Moran's I values for analysis [30].

Results

LER Identification in HTNP and its Surrounding Areas

Fig. 1 presents the spatial distribution of LER surrounding HTNP from 2002 to 2022 and reveals significant trends in ecological degradation and recovery, with implications for long-term conservation planning. The maps presented in this study illustrate the shifting risk patterns in the region, based on the classification of areas into five risk categories: "Lowest Risk", "Lower Risk", "Medium Risk", "Higher Risk", and "Highest Risk".

The series of maps from 2002 to 2022 demonstrates the evolution of LER, with marked shifts occurring in both the extent and intensity of risk across the study area. In 2002, a substantial portion of the area was classified as "Higher Risk" and "Highest Risk," particularly in the coastal and heavily developed regions, reflecting the pressures of urbanization, land-use change, and industrialization. Over the following two decades, the ecological risks in these regions intensified, with the "Highest Risk" zones expanding in line with increasing human activities. In contrast, some inland areas experienced a decrease in ecological risk, with "Lowest Risk" and "Lower Risk" zones becoming more prominent, suggesting the positive effects of conservation and restoration efforts.

Notably, the "Highest Risk" zones in the coastal areas have expanded over time, reflecting the intensification of human activities such as urbanization, agricultural expansion, and infrastructure development. These areas, characterized by high population density and land use intensity, face significant ecological pressures, including habitat loss, fragmentation, and reduced connectivity between natural habitats. In contrast, the interior regions of the national park and its surrounding buffer zones have shown a steady decline in ecological risk, with

Table 3. Evaluation System and Weighting of Ecological Sensitivity in the Surrounding Areas of HTNP.

Normative layer	Evaluation factor	Ecological sensitivity classification				
		(1)	(2)	(3)	(4)	(5)
Geological feature	DEM (m)	0-20	20-40	40-60	60-80	>80
	Slope (°)	45-90	30-45	25-30	15-25	0-15
	Aspect	Due North	Northeast, northwest	Due east, Due west	Southeast, southwest	Due south, Flat land
Underground water system	Waters	0-200	200-500	500-800	800-1000	>1000
Surface vegetation	NDVI	0.75-1	0.65-0.75	0.5-0.65	0.35-0.5	0-0.35
Human activity	lucc	Wetlands, forests	water bodies	Shrubs, grass	cropland	other
LER	LER	Level 1 risk	Secondary risks	Medium risk	high risk	Ultra-high risk
Value		1	2	3	4	5

areas shifting towards "Lower Risk" categories, which could be attributed to effective conservation practices, including the establishment of protected areas and ecological restoration programs.

The "Change in 2002-2022" map provides a comparative analysis of the spatiotemporal shifts in ecological risk across the region. The results highlight areas of increasing and decreasing ecological risk, which are pivotal for understanding the long-term sustainability of the region's ecosystems. The "Highest Risk Increase Zones" are primarily concentrated along the coast and in regions with intense human activity, whereas "Lowest Risk Reduction Zones" are more common in the inner buffers and areas subject to active conservation measures. These findings suggest that the conservation policies implemented within the national

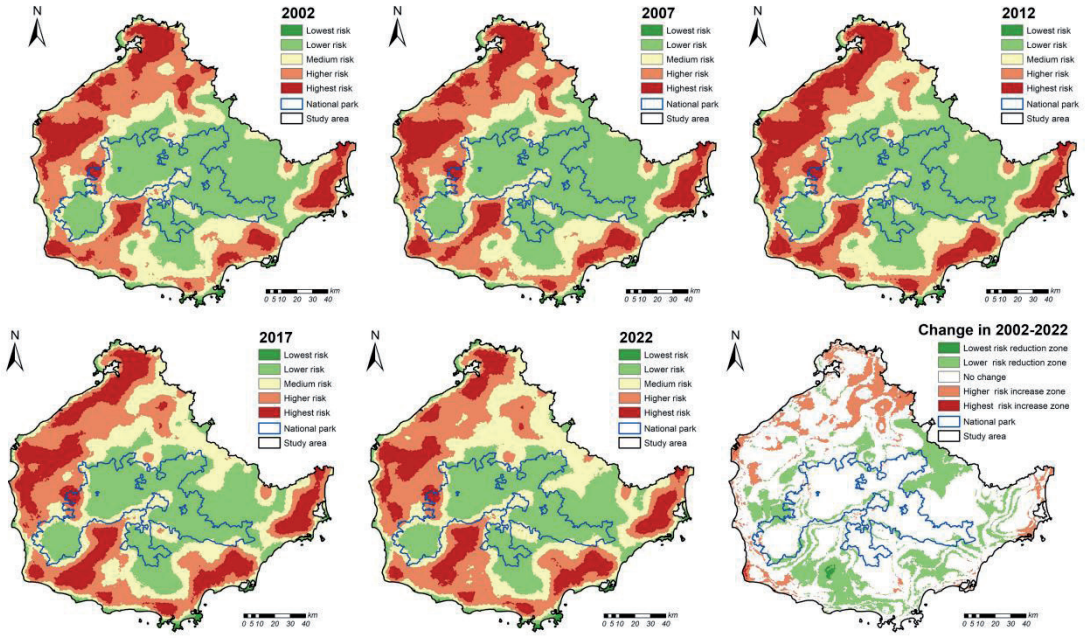

Fig. 1. Temporal changes in LER in HTNP and surrounding areas (2002–2022). This figure presents the spatial distribution of ecological risk levels in the study area from 2002 to 2022, with risk levels classified into five categories: "Lowest Risk", "Lower Risk", "Medium Risk", "Higher Risk", and "Highest Risk".

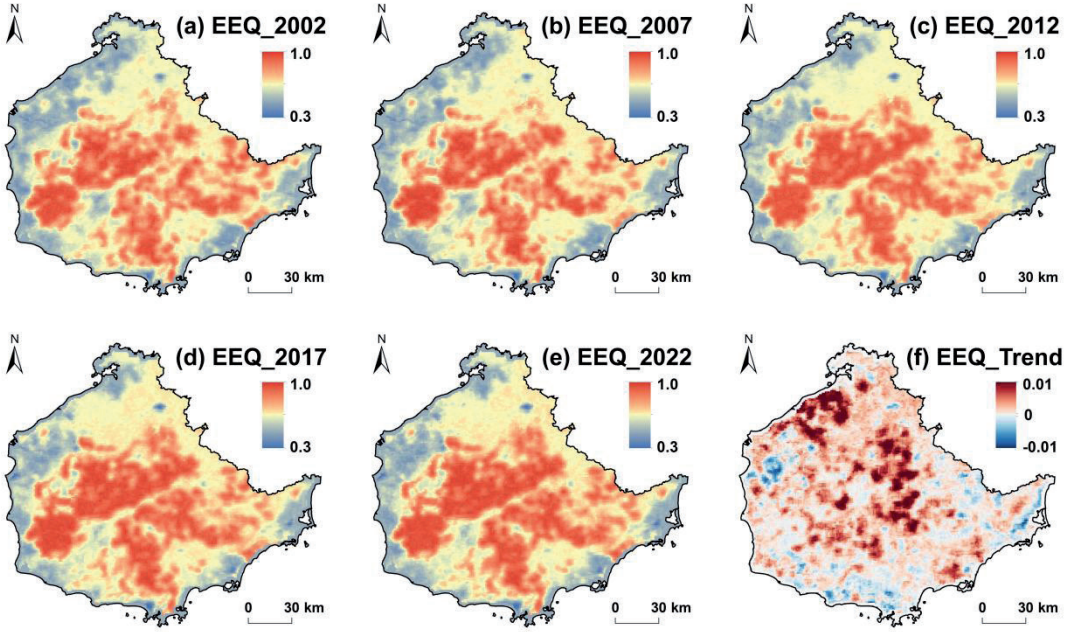

Fig. 2. Spatiotemporal dynamics of EEQ in HTNP and surrounding areas (2002-2022).

park's core and its immediate buffer zones have been relatively successful in mitigating ecological risk, but more attention is needed in the periphery to counteract growing anthropogenic pressures.

The findings of this study underscore the need for adaptive conservation strategies tailored to the spatial and temporal dynamics of ecological risk. The expanding "Highest Risk" zones necessitate immediate action to address urban sprawl, unsustainable land use, and habitat fragmentation. Conversely, the positive trends observed in the inland and core park areas should be maintained and expanded. Expanding buffer zones, improving landscape connectivity, and enhancing ecological corridors between the park's core and its surroundings are essential strategies to ensure the long-term viability of the Hainan Tropical Rainforest ecosystem.

Analysis of EEQ in HTNP and its Surrounding Areas

Fig. 2 presents the spatial distribution of EEQ in HTNP and its surrounding buffer zones for the years 2002, 2007, 2012, 2017, and 2022, as shown in panels (a) through (e). The maps use a color gradient, where blue represents the lowest risk, yellow denotes medium risk, and red indicates the highest risk.

From 2002 to 2022, a notable improvement in the overall ecological quality was observed, especially within the national park's core areas. In 2002 (panel a), large sections of the study area exhibited medium-to-high ecological risk, with much of the landscape in the higher risk categories. By 2007 (panel b), there were signs of improvement in the central region, with an expansion of lower-risk areas. The trend continued through 2012 and 2017 (panels c and d), with a significant shift towards improved ecological conditions, particularly in the core area of the park. By 2022 (panel e), the central zone largely falls into the "Lowest Risk" category, reflecting substantial ecological recovery.

Panel (f) illustrates the trend of change in EEQ from 2002 to 2022. This trend map highlights areas with significant increases in EEQ (marked in red and orange) and those with stagnation or decline (indicated in blue). The trend analysis shows that while the core national park area has benefited from successful conservation efforts, the outer buffer zones show mixed trends, with some areas continuing to experience ecological stress, possibly due to human-induced factors such as land use change and development activities.

These findings underscore the importance of ongoing, targeted conservation measures, particularly in the buffer zones, to ensure the sustainability of ecological improvements and to mitigate further degradation in vulnerable areas surrounding the national park.

Construction of ESPs in HTNP and its Surrounding Areas

Fig. 3 illustrates the evolution of ESPs, specifically ecological corridors, around HTNP for the years 2002, 2007, 2012, 2017, and 2022, as shown in panels (a) to (e). The ecological sources, identified through the highest quality ecological environments based on a natural breaks classification, are shown in green.

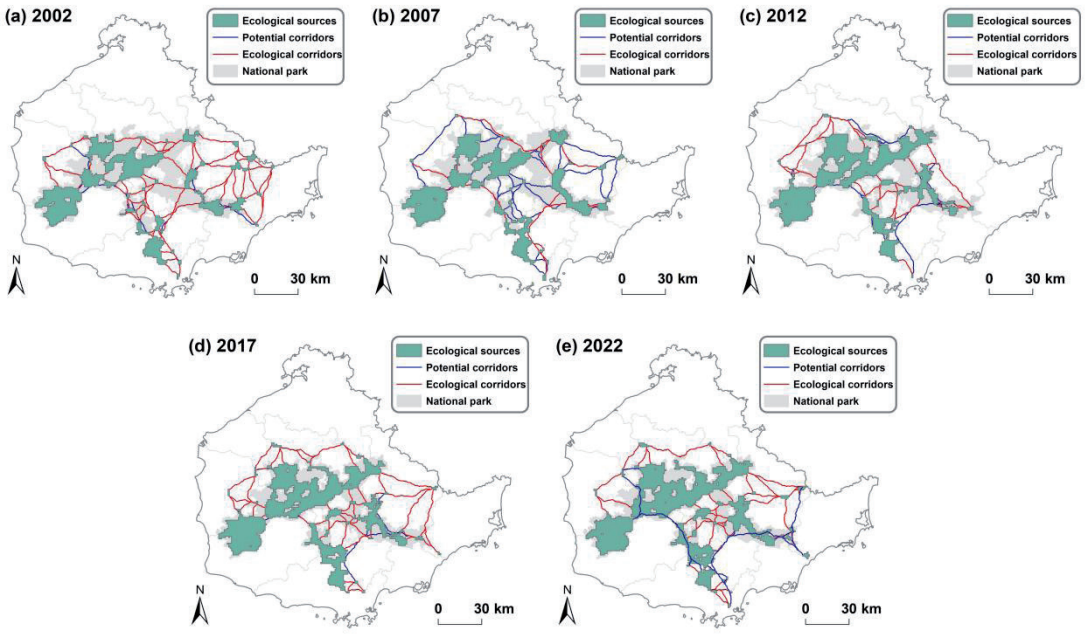

Fig. 3. Evolution of ESPs in HTNP and surrounding areas (2002-2022): spatial distribution changes of primary ecological corridors (Red) and potential ecological corridors (Blue).

These ecological sources represent the most important areas for biodiversity preservation. The ecological corridors, depicted in red, indicate established pathways that connect ecological sources, ensuring ecological connectivity across the landscape. Additionally, the potential corridors, represented in blue, show areas that could serve as potential connectivity routes if landscape management strategies are enhanced.

The methodology for the identification of ecological sources involved evaluating various resistance factors, including Digital Elevation Models (DEM), slope, aspect, water availability, Normalized Difference Vegetation Index (NDVI), land use/land cover (LUCC) data, and LER, all of which were processed using the natural breaks method. These resistance factors play a crucial role in determining the cost of movement for species and the permeability of the landscape. The Maximum Connectivity Risk (MCR) model was applied to assess ecological corridor connectivity and to derive the final security pattern.

The temporal evolution of ESPs surrounding HTNP (2002-2022) demonstrates a marked improvement in landscape connectivity and ecological integrity. Over the two decades, the establishment of ecological corridors and sources, as well as the expansion of potential corridors, reflects the increasing effectiveness of conservation strategies. The primary ecological corridors, indicated in red, have progressively extended from the park's core, forming an interconnected network that enhances ecological resilience across the landscape. The potential corridors (blue) also show significant growth, further strengthening connectivity between fragmented habitats and providing future opportunities for biodiversity movement.

Throughout the study period, the network of ecological sources (green) has expanded, particularly within areas adjacent to the national park, signifying successful habitat restoration and conservation initiatives. The strategic development of these sources, along with the increased density of both primary and potential corridors, highlights the positive impact of long-term ecological planning and restoration efforts. However, the changes also reveal that some peripheral areas, particularly in the northeast, still face challenges in connectivity, pointing to the need for continued conservation efforts in these zones.

Notably, the period from 2007 to 2017 saw the most significant increase in ecological connectivity, with large portions of the landscape transitioning to higher connectivity levels. This phase marks the critical expansion of primary corridors, which have linked previously isolated ecosystems, thus enhancing the overall health and functionality of the landscape. The 2022 map shows a well-integrated network of corridors, establishing a robust ecological framework for maintaining biodiversity and ecosystem services.

The change map for 2002-2022 further highlights these improvements, illustrating the shift from lower to higher connectivity zones, especially in areas with low human disturbance. These findings underscore the importance of ecological corridors in mitigating fragmentation, promoting biodiversity conservation, and ensuring the long-term sustainability of the Hainan Tropical Rainforest ecosystem. While substantial progress has been made, there is a continued need for targeted conservation efforts, particularly in the less-connected regions, to fully integrate the landscape and protect its ecological function.

Discussion

Policy Implications

In the context of an intensifying global ecological crisis, ecological security and sustainable development have become core concerns of the international community [31]. As a national pilot zone for ecological civilization, the protection of Hainan's tropical rainforests has been given high priority and comprehensively advanced by the Chinese government. In January 2019, China approved the Hainan Provincial Tropical Rainforest National Park System Pioneer Area Program [32], which provided clear guidance for the program's construction. In the same year, a dedicated management authority was established, and strict land-use control and ecological restoration policies were implemented [33]. These measures included delineating ecological redlines, adjusting land-use zoning, and reforming the forest property rights system, with the aims of restricting development, curbing the expansion of impervious surfaces, reducing agricultural encroachment, restoring degraded land, enhancing landscape connectivity, and mitigating ecological risks.

However, a comparison of the spatial distributions of the EEQ Index and the LER Index indicates that some high-risk areas, despite being under policy control, have shown limited ecological improvement [34]. For instance, the agricultural reclamation area in the northeast and the coastal construction expansion zone in the southeast [35] have experienced below-average improvements in ecological quality alongside continuous increases in ecological risk. This reflects the heightened vulnerability of local ecosystems and reveals a significant time lag between policy implementation and ecological feedback, underscoring the urgent need for high-precision spatial monitoring and risk early-warning systems.

Ecological corridor identification and connectivity analysis [36] indicate that a structural network has begun to form among ecological source areas within the national park, with major corridors extending around the core zone and effectively supporting the continuity of ecological processes. Nevertheless, corridors in peripheral regions – particularly those with diverse land-use types and high development intensity – display a "fragment-island" pattern and low ecological

connectivity. This suggests that the current ESP lacks spatial balance and systematic integration, especially across administrative boundaries and in high-resistance zones, where the stability and accessibility of ecological networks require further improvement.

Empirical evidence shows that inadequate supervision and enforcement in certain townships have reduced ecological corridor stability and exacerbated fragmentation [37], highlighting the need to optimize policy design. It is therefore recommended that, building on existing ecological protection policies, the ESP evolve into a multi-level system of "core protection–transition coordination–peripheral buffering". Priority should be given to ecological restoration and functional reconstruction in high-risk patches and potential corridors, based on ecological connectivity assessments, to enhance the integrity of the ecological network. For areas with high ecological risk, a differentiated management mechanism based on spatial sensitivity should be introduced [38], along with targeted, time-sensitive ecological compensation and land-use adjustment strategies in zones where special forest land and construction land are interspersed, in order to alleviate the obstructive effects of land-use conflicts on ecological connectivity.

Furthermore, the use of high-frequency remote sensing imagery and GIS-based dynamic analysis can establish a "policy–ecological response" feedback mechanism to quantify the strength and lag time of different policy interventions across ecological units. Although national and regional ecological policies have provided a foundational framework for the ESP of HTNP, a shift toward a spatially differentiated governance system – featuring rigid ecological controls, flexible restoration mechanisms, and dynamic coordination strategies – is necessary. Such a system, supported by adaptive adjustments based on multi-source spatial data, is essential to fully enhance ecosystem resilience and the capacity for regional sustainable development.

Limitations and Future Prospects

Although this study constructed a multi-level ESP for HTNP and its surrounding areas using multi-source remote sensing data [39], GIS analysis [40], and landscape ecology theory [41, 42], several limitations remain. First, the remote sensing imagery spans 2002-2022; however, the limited spatial and temporal resolution of the earlier data may fail to capture short-term drastic changes or small-scale ecological disturbances, particularly in areas with frequent agricultural activities or abrupt land-use transitions. This limitation may affect the precision of the data and the temporal accuracy of ecological risk assessments. Second, in constructing the LER index [43], although key structural indicators – such as fragmentation, dominance, and separation – were included, non-structural ecological variables, including the intensity of anthropogenic disturbance and the degradation of ecosystem services, were not fully considered. Furthermore, in ecological corridor identification [44], the MCR model assumes that species migration paths are determined solely by resistance surfaces, without accounting for behavioral heterogeneity, habitat preferences, or functional compensation relationships among ecosystems.

Future studies could address these limitations in several ways:

(1) Enhance and diversify quantitative analysis methods to evaluate the impacts of relevant policies, socio-economic indicators, and anthropogenic trajectory data on local ecosystems, assess the coordinating effects and extent of these impacts, and improve the sensitivity of risk indices to human disturbances.

(2) Strengthen human–land system analysis by increasing the spatial and temporal resolution of multi-source remote sensing data and integrating multi-scale datasets for dynamic monitoring.

(3) Improve the spatial availability of policy implementation data and advance the quantitative modeling of ecological and land-source policies to establish an ESP assessment framework with greater universality, precision, and dynamic adaptability.

Conclusions

This study conducts a correlation analysis between ecological sensitivity and landscape patterns, integrating ecological quality assessment, LER analysis, and minimum cumulative resistance (MCR) modeling to systematically construct a multilevel ESP for HTNP and its surrounding areas. Using multi-source remote sensing data, GIS technology, and ecological sensitivity assessment, we comprehensively examined the spatial and temporal evolution of landscape fragmentation, ecological vulnerability, and environmental quality from 2002 to 2022.

The results indicate that:

(1) Spatially, the core area of HTNP has maintained gradual and stable ecological conditions, largely due to strict ecological protection policies. In contrast, surrounding areas exhibit elevated ecological risks and pronounced spatial heterogeneity as a result of land-use change, agricultural expansion, and human disturbance. These findings confirm the effectiveness of current conservation measures within the park, while highlighting the urgent need to extend protection efforts beyond park boundaries to maintain regional ecological integrity and ensure the long-term sustainability of ecosystem services.

(2) Temporally, the ecological safety network of HTNP expanded outward from the core area over the 20-year period, forming an interconnected structure that facilitated the identification and optimization of ecological corridors through the MCR model. This expansion significantly improved landscape connectivity, enhanced ecological mobility, and increased species

migration potential, thereby fostering a more resilient ESP. Nevertheless, persistent fragmentation in high-risk zones underscores the necessity for targeted corridor restoration and habitat rehabilitation.

In conclusion, the ecological security system developed in this study – combining strict control measures, adaptive restoration mechanisms, and dynamic coordination strategies – plays a critical role in ensuring the long-term ecological sustainability of HTNP. The proposed framework not only supports the sustainable management of HTNP but is also applicable to other national parks with similar ecological sensitivity. By integrating scientific approaches, this system makes an important contribution to global discussions on biodiversity conservation and the enhancement of ecological resilience.

Conflict of Interest

The authors declare no conflict of interest.

References

1. DEBINSKI D.M., HOLT R.D. A survey and overview of habitat fragmentation experiments. Conservation biology. **14** (2), 342, **2000**.
2. DORNER B., LERTZMAN K., FALL J. Landscape pattern in topographically complex landscapes: issues and techniques for analysis. Landscape Ecology. **17** (8), 729, **2002**.
3. BAORONG H., YI W., LIYANG S., CONGLIN Z., DUOWEI C., JING S., SIYUAN H. Pilot programs for national park system in China: Progress, problems and recommendations. Bulletin of Chinese Academy of Sciences. **33** (1), 76, **2018** [In Chinese].
4. WANG C., YU C., CHEN T., FENG Z., HU Y., WU K. Can the establishment of ecological security patterns improve ecological protection? An example of Nanchang, China. Science of the Total Environment. **740**, 140051, **2020**.
5. PICKETT S.T., CADENASSO M.L. Landscape ecology: spatial heterogeneity in ecological systems. Science. **269** (5222), 331, **1995**.
6. LI W., KANG J., WANG Y. Exploring the interactions and driving factors among typical ecological risks based on ecosystem services: A case study in the Sichuan-Yunnan ecological barrier area. Ecological Indicators. **170**, 113000, **2025**.
7. BAGUETTE M., BLANCHET S., LEGRAND D., STEVENS V.M., TURLURE C. Individual dispersal, landscape connectivity and ecological networks. Biological Reviews. **88** (2), 310, **2013**.
8. MITCHELL M.G., SUAREZ-CASTRO A.F., MARTINEZ-HARMS M., MARON M., MCALPINE C., GASTON K.J., JOHANSEN K., RHODES J.R. Reframing landscape fragmentation's effects on ecosystem services. Trends in Ecology & Evolution. **30** (4), 190, **2015**.
9. DE LANGE H.J., SALA S., VIGHI M., FABER J.H. Ecological vulnerability in risk assessment – A review and perspectives. Science of the Total Environment. **408** (18), 3871, **2010**.
10. LI X., LI S., ZHANG Y., O'CONNOR P.J., ZHANG L., YAN J. Landscape ecological risk assessment under multiple indicators. Land. **10** (7), 739, **2021**.
11. LEUVEN R.S., POUDEVIGNE I. Riverine landscape dynamics and ecological risk assessment. Freshwater Biology. **47** (4), 845, **2002**.
12. XU W., WANG J., ZHANG M., LI S. Construction of landscape ecological network based on landscape ecological risk assessment in a large-scale opencast coal mine area. Journal of Cleaner Production. **286**, 125523, **2021**.
13. HU X., XU H. A new remote sensing index for assessing the spatial heterogeneity in urban ecological quality: A case from Fuzhou City, China. Ecological Indicators. **89**, 11, **2018**.
14. ZHANG Y., ZHANG C., ZHANG X., WANG X., LIU T., LI Z., LIN Q., JING Z., WANG X., HUANG Q. Habitat quality assessment and ecological risks prediction: an analysis in the Beijing-Hangzhou Grand Canal (Suzhou Section). Water. **14** (17), 2602, **2022**.
15. SASAKI T., FURUKAWA T., IWASAKI Y., SETO M., MORI A.S. Perspectives for ecosystem management based on ecosystem resilience and ecological thresholds against multiple and stochastic disturbances. Ecological Indicators. **57**, 395, **2015**.
16. TINGHUI M. Nature and environment of the Hainan Province of China. Kyoto University of Education Environmental Education Research Annual Report/Annual Report of Environmental Education Research at Kyoto University of Education. **17**, 141, **2009**.
17. LI L., TANG H., LEI J., SONG X. Spatial autocorrelation in land use type and ecosystem service value in Hainan Tropical Rain Forest National Park. Ecological Indicators. **137**, 108727, **2022**.
18. WEI L., LI M., MA Y., WANG Y., WU G., LIU T., GONG W., MAO M., ZHAO Y., WEI Y. Construction of an Ecological Security Pattern for the National Park of Hainan Tropical Rainforest on the Basis of the Importance of the Function and Sensitivity of Its Ecosystem Services. Land. **13** (10), 1618, **2024**.
19. HAN N., YU M., JIA P., ZHANG Y., HU K. Influence of Human Activity Intensity on Habitat Quality in Hainan Tropical Rainforest National Park, China. Chinese Geographical Science. **34** (3), **2024**.
20. HAINES-YOUNG R., CHOPPING M. Quantifying landscape structure: a review of landscape indices and their application to forested landscapes. Progress in Physical Geography. **20** (4), 418, **1996**.
21. LI J., PENG X., TANG R., GENG J., ZHANG Z., XU D., BAI T. Spatial and temporal variation characteristics of ecological environment quality in China from 2002 to 2019 and influencing factors. Land. **13** (1), 110, **2024**.
22. HERBEI M.V., CIOLAC V., ŞMULEAC A., NISTOR E., CIOLAC L. Georeferencing of topographical maps using the software ARCGIS. Research Journal of Agricultural Science. **42** (3), 595, **2010**.
23. YANG X., YAN L., ZENG L. How to handle uncertainties in AHP: The Cloud Delphi hierarchical analysis. Information Sciences. **222**, 384, **2013**.
24. LI J., PENG X., LI C., LUO Q., PENG S., TANG H., TANG R. Renovation of traditional residential buildings in Lijiang based on AHP-QFD methodology: A case study of the Wenzhi Village. Buildings. **13** (8), 2055, **2023**.
25. YE H., YANG Z., XU X. Ecological corridors analysis based on MSPA and MCR model – A case study of the

Tomur World Natural Heritage Region. Sustainability. **12** (3), 959, **2020**.
26. WEI Q., HALIKE A., YAO K., CHEN L., BALATI M. Construction and optimization of ecological security pattern in Ebinur Lake Basin based on MSPA-MCR models. Ecological Indicators. **138**, 108857, **2022**.
27. ANSELIN L. Local spatial autocorrelation. Other Local Spatial Autocorrelation Statistics. **711**, **2020**.
28. O'NEILL R.V., KRUMMEL J.R., GARDNER R.E.A., SUGIHARA G., JACKSON B., DEANGELIS D., MILNE B., TURNER M.G., ZYGMUNT B., CHRISTENSEN S. Indices of landscape pattern. Landscape Ecology. **1** (3), 153, **1988**.
29. ZHOU Z., LI J. The correlation analysis on the landscape pattern index and hydrological processes in the Yanhe watershed, China. Journal of Hydrology. **524**, 417, **2015**.
30. CUI L., ZHAO Y., LIU J., HAN L., AO Y., YIN S. Landscape ecological risk assessment in Qinling Mountain. Geological Journal. **53**, 342, **2018**.
31. LIU C., LI W., XU J., ZHOU H., LI C., WANG W. Global trends and characteristics of ecological security research in the early 21st century: A literature review and bibliometric analysis. Ecological Indicators. **137**, 108734, **2022**.
32. TANG X. The establishment of national park system: A new milestone for the field of nature conservation in China. International Journal of Geoheritage and Parks. **8** (4), 195, **2020**.
33. ZONG L. The path to effective national park conservation and management: Hainan tropical rainforest National Park System Pilot Area. International Journal of Geoheritage and Parks. **8** (4), 225, **2020**.
34. HUANG X., WANG X., ZHANG X., ZHOU C., MA J., FENG X. Ecological risk assessment and identification of risk control priority areas based on degradation of ecosystem services: A case study in the Tibetan Plateau. Ecological Indicators. **141**, 109078, **2022**.
35. XU Y., PU L., ZHANG R., ZHU M., ZHANG M., BU X., XIE X., WANG Y. Effects of agricultural reclamation on soil physicochemical properties in the mid-eastern coastal area of China. Land. **10** (2), 142, **2021**.
36. SALVIANO I.R., GARDON F.R., DOS SANTOS R.F. Ecological corridors and landscape planning: a model to select priority areas for connectivity maintenance. Landscape Ecology. **36** (11), 3311, **2021**.
37. MA J., LI L., JIAO L., ZHU H., LIU C., LI F., LI P. Identifying ecological security patterns considering the stability of ecological sources in ecologically fragile areas. Land. **13** (2), 214, **2024**.
38. DING X., ZHOU C., ZHONG W., TANG P. Addressing uncertainty of environmental governance in environmentally sensitive areas in developing countries: a precise-strike and spatial-targeting adaptive governance framework. Sustainability. **11** (16), 4510, **2019**.
39. HE C., GAO B., HUANG Q., MA Q., DOU Y. Environmental degradation in the urban areas of China: Evidence from multi-source remote sensing data. Remote Sensing of Environment. **193**, 65, **2017**.
40. MAGUIRE D.J. An overview and definition of GIS. Geographical information systems: Principles and applications. **1** (1), 9, **1991**.
41. NAVEH Z., LIEBERMAN A.S. Landscape ecology: theory and application. Springer Science & Business Media, **2013**.
42. ZHOU G., HUAN Y., WANG L., ZHANG R., LIANG T., HAN X., FENG Z. Constructing a multi-leveled ecological security pattern for improving ecosystem connectivity in the Asian water Tower region. Ecological Indicators. **154**, 110597, **2023**.
43. ZHANG W., CHANG W. J., ZHU Z. C., HUI Z. Landscape ecological risk assessment of Chinese coastal cities based on land use change. Applied Geography. **117**, 102174, **2020**.
44. WU X., PAN J., ZHU X. Optimizing the ecological source area identification method and building ecological corridor using a genetic algorithm: A case study in Weihe River Basin, NW China. Ecological Informatics. **80**, 102519, **2024**.